

Effects of Global Warming on the Average Wind Speed Field in Central Japan

Mustamin Rahim^{1,2,*}, Jun Yoshino², Yasuhiro Doi³ and Takashi Yasuda⁴

¹Department of Architecture, Faculty of Engineering, Khairun University, Indonesia

²Graduate School of Environmental and Renewable Energy Systems, Gifu University, Japan

³Penta-Ocean Construction Co., Ltd., Japan

⁴Aichi University of Technology, Japan

*Corresponding author: mustamin_rahim@yahoo.co.id

Abstract: The authors compare distributions of annual mean wind speed during 1961–2099 at altitudes of 30–100 m above ground level (AGL) in Central Japan based on several available databases. Wind speed fields are statistically interpolated in time and space using three existing databases: the 333-m resolution local wind field database in Central Japan during 2001–2002 (GWA333), the global reanalysis ECMWF during 1957–2001 (ERA40), and the global multi-model database during 2000–2100 (CMIP3) under the SRES A1B scenario. The interpolated data is validated by available surface observation conducted by the Japan Meteorological Agency, and we confirm that the interpolation shows good agreement with the observations.

Results show that domain-averaged wind speeds in 2099 evaluated by the statistical interpolation exceed the wind speeds in 2001 evaluated by GWA333 by about 0.48 m/s at 30 m AGL. Over the coastal and mountainous regions, the wind speed at 30 m AGL increase from 8 m/s in 2001 to 10 m/s in 2099. The gradual increase of the surface wind speed might be completed until the early 21st century. It is concluded that if global warming advances according to the IPCC A1B scenario, the surface wind speed, namely, the wind energy resource in Central Japan is expected to increase gradually during the early 21st century.

Keywords: average wind speed, wind energy, global warming.

1. Introduction

Fossil fuels, which will continue to dominate global energy usage, will account for around 85% of the increase in world primary demand during 2002–2030. Furthermore, their share in total demand will increase slightly from 80% in 2002 to 82% in 2030. The share of renewable energy sources will remain flat at around 4%, while that of nuclear power is expected to drop from 7% to 5% [1]. Oil energy resources will be increasingly scarce and expensive.

An important problem is the combustion of fossil fuels to generate electricity. It produces atmospheric CO₂ emissions. In 2005, total CO₂ emissions were 26.6 billion tons. More than 41% were produced from fossil fuels. That figure is expected to increase to 46% by 2030, generating CO₂ in large amounts, and releasing it to the atmosphere as the primary cause of global warming [2-3].

Fossil fuel utilization presents severe environmental impacts. They can be reduced by replacement of fossil fuels with renewable energy sources such as wind energy. The Kyoto Protocol is part of the United Nations Framework Convention on climate change. Its main objective is to extract a firm commitment from developed countries for reducing their greenhouse gas emissions [4–6]. The advancement of renewable energy technologies seems to present a viable solution for environmental problems produced by other energy sources.

The wind energy potential of the earth is huge. It is sufficient, in principle, to meet all the world's electricity needs. Virtually every country has sites with average wind speeds of more than 5 m/s measured at 10 m altitude, which are sufficiently strong winds to enable their development as a resource [7]. Among renewable sources of energies, wind energy is an important source of environmentally friendly energy that has become more important in recent years [8]. For the evaluation of productivity of specific plants and the relative technical-economic considerations, detailed wind field databases are required, such as data acquired over long periods of time [9].

Wind speed and air density greatly influence wind power generation. Wind conditions are strongly related to local

weather conditions and geographical locations, so that the potential of wind power generation differs in each site. Several studies on global warming impacts indicate that rising temperatures might decrease surface wind speed [10-13]. Therefore, this study specifically analyzes the relation of global warming on wind speed field in Central Japan, using three available databases to compensate for each their limitations. Details of the database interpolations are described in Section 2. Section 3 presents the high resolution of wind speed fields in past and future to evaluate effects of global warming on the surface wind speed, and also discusses seasonal wind speed change to quantify its contribution to the annual wind speed changes. Conclusions are given in section 4.

2. Experimental

Surface wind speeds are strongly influenced by surrounding topography and synoptic-scale weather conditions. Steep mountains and complex terrain in Japan require the use of high-resolution databases to estimate local wind speeds accurately. Recently, several kinds of databases for wind energy assessment have become available, although problems remain related to the spatial resolution and the time period availability. Therefore, we statistically interpolate a long term wind speed fields in time and space using three existing databases: the 333-m resolution local wind field database in Central Japan (Figure 1) during 2001–2002 developed by Gifu University (hereafter called GWA333) [14], the ECMWF global atmospheric reanalysis during 1957–2001 (hereafter called ERA40) [15], and the global atmospheric multi-model database under the SRES A1B scenario during 2000–2100 (hereafter called CMIP3) [16-17]. The condition of wind field database can be seen in Table 1.

GWA333 is dynamically analyzed by using the mesoscale meteorological model PSU/NCAR MM5 [18] and the mass-consistent wind field model [14], and has the advantage of having a high-resolution wind field during a one-year period. Although ERA40 and CMIP3 are simulated by lower-resolution general circulation models with available observations and future-climate

Table 1. The details of the wind field database, GWA333, ERA40, and CMIP3.

| | GWA333 High-resolution local wind field database of Gifu University | ERA40 Global reanalysis of ECMWF | CMIP3 Global multi-model database of Intercomparison Proj. phase 3 (A1B Scenario) |
|----------------------|---|--|--|
| Period | 2001-2002 | 1957-2001 | 2000-2100 |
| Computational Domain | Central Japan | Global | Global |
| Developer | Gifu University | European Centre for Medium Range Weather Forecasts (ECMWF) | World Climate Research Programme (WCRP) |
| Spatial Resolution | 333 m | 2.5 deg | 1-5 deg |
| Vertical Resolution | 30-100 m (5 layers) | 1000-1 hPa (23 layers) | 1000-1 hPa |
| Time Interval | Hourly | Monthly | Monthly |
| Data Types | Wind direction and wind speed, | Wind direction, wind speed, temperature, humidity, etc. | Wind direction, wind speed, temperature, humidity, etc. |



Figure 1. Maps of the study area.

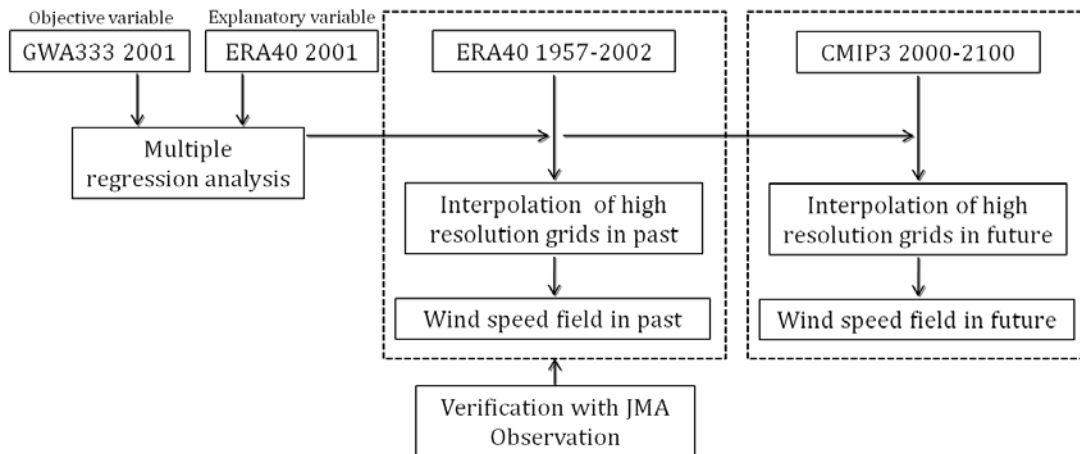


Figure 2. Flowchart of the study.

scenarios respectively, they have the advantage of having very long-term and physically consistent estimates of large-scale meteorological fields. The authors statistically analyze the average surface wind speed with such a high-resolution grid as GWA333 according to regression equations correlated with the 850-hPa wind field derived from ERA40 and CMIP3. This is because the surface wind field is strongly affected by the upper-level wind and surrounding complex topography. These statistically-merged datasets would compensate for the limitations of each dataset.

The flow of the statistical estimation used in this study is seen in Figure 2. Multiple regression equation representing the relationship between upper and surface winds is expressed as the following equation,

$$y = a + bx_1 + cx_2 + dx_3 + \dots \quad (1)$$

where: y is the objective variable which is equivalent to surface wind fields obtained from GWA333. a , b , and c are regression coefficients. x_1 , x_2 , and x_3 are explanatory variables which is equivalent to upper-level atmospheric conditions derived from

ERA40. It should be noted that both of GWA333 and ERA40 are available during one year period in 2001. The following three combinations of explanatory variables are tested in this study.

Case 1:

$$|\bar{V}|_{surface} = a + b|\bar{V}| \tag{2}$$

Case 2:

$$|\bar{V}|_{surface} = a + b|\bar{V}| + c\bar{\theta} \tag{3}$$

Case 3:

$$|\bar{V}|_{surface} = a + b|\bar{V}| + c \frac{\sqrt{u^{-2} + v^{-2}}}{|\bar{V}|} \tag{4}$$

where, $|\bar{V}|_{surface}$ is the monthly-averaged surface wind speed. $|\bar{V}|$ is the monthly-averaged wind speed at 850 hPa. $\bar{\theta}$ is the monthly-averaged potential temperature at 850 hPa. $\frac{\sqrt{u^{-2} + v^{-2}}}{|\bar{V}|}$ is the monthly-averaged wind direction change parameter at 850 hPa. Based on the verification result, the combination of $|\bar{V}|$ and $\frac{\sqrt{u^{-2} + v^{-2}}}{|\bar{V}|}$ in Case 3 show the highest correlation with the surface observations obtained by the Japan Meteorological Agency (see in Figure 3). Thus, the multiple regression equation represented by equation (4) is applied to estimate the monthly-averaged surface wind speed with a high-resolution grid used in GWA333, and the long-term and high-resolution database containing the surface wind fields under the future climate condition is constructed based on the regression coefficients defined by ERA40 and the explanatory variables given from CMIP3.

3. Results and Discussion

Figure 4 presents the spatial distributions of wind speeds at altitudes of 30 m and 100 m above ground level

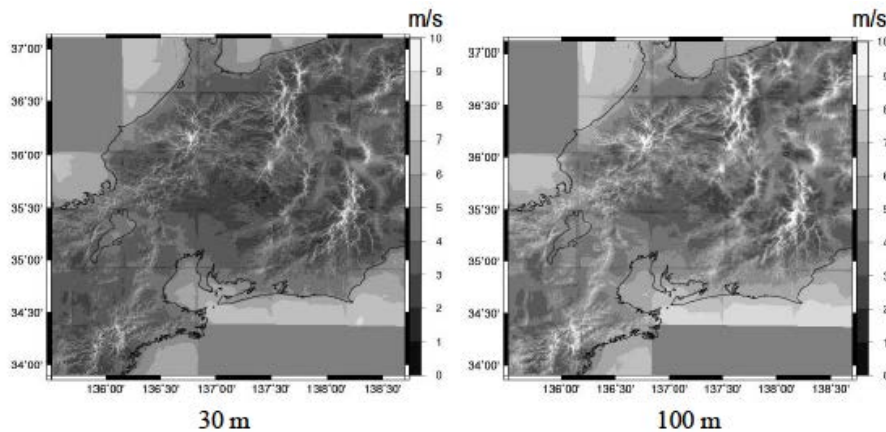


Figure 4. Spatial distributions of average wind speed during 1961-2001 at 30 m and 100 m AGL.

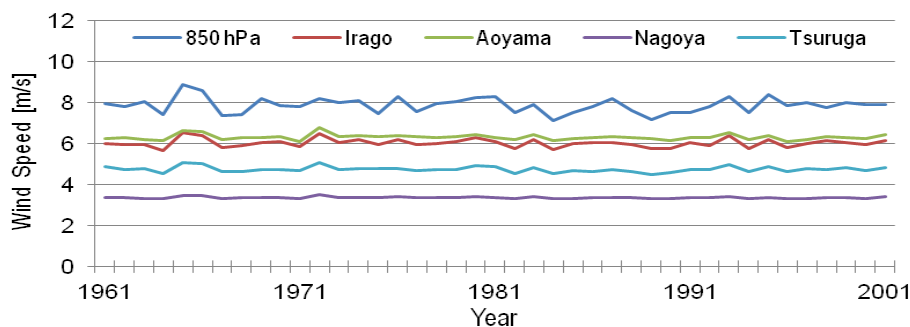


Figure 5. Time series of annual average wind speed on surface and 850 hPa during 1961-2001.

(AGL) averaged during 1961-2001 based on GWA333 and ERA40. The annual wind speeds vary at each location from 2 m/s to 10 m/s. The highest wind speed occurs in coastal and highland areas: over 8 m/s. Valley areas produce the lowest wind speeds of about 2 m/s. However, comparison of the wind speed distributions at 30 m and 100 m AGL shows higher wind speeds at higher altitudes. Dominant wind speeds are about 5 m/s at 30 m AGL and higher than 7 m/s at 100 m AGL.

Figure 5 presents time series of the annual average wind speeds on surface and 850 hPa during 1961-2001 estimated by GWA333 along with ERA40 at the 850-hPa level at the grid point of 35.0°N, 137.5°E. Wind speeds at the surface are lower than those of ERA40 at 850 hPa at 35.0°N, 137.5°E, owing to the effect of surface friction, and differ among locations. The highest surface wind speed is measured in Aoyama: around 8 m/s. The lowest surface wind speed is observed in Nagoya: around 3.5 m/s. Generally, the wind speed is higher than 5 m/s except in the Nagoya area where its large roughness length reduces the wind speed at the surface. Wind speed fluctuations year by year are not large throughout the 40-year period in the four locations. This is because wind speed fluctuations at 850-hPa are not large during 40-year period.

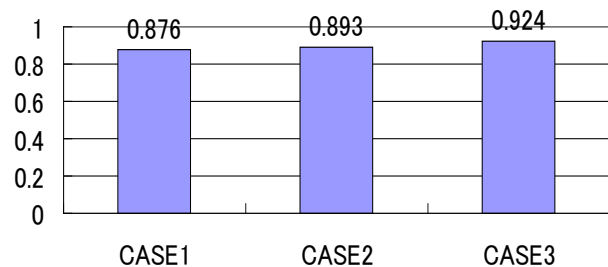


Figure 3. Correlation of explanatory variables in each case.

Figure 6 presents the spatial distributions of the annual average wind speed at 30 m AGL in 1961, 1981, and 2001. Spatial distribution shows that the wind speed fields are similar in each year from 2 m/s to 8 m/s. It indicates that change of the surface wind speed before 2001 is not apparent in Central Japan. Figure 7 presents the spatial distributions of the averaged wind speed difference at 30 m AGL and 100 m AGL between 1960's decade and 1990's decade, indicating that the temporal change of the surface wind speed is not so significant during the late 20th century. Areas experiencing wind speed reduction are wider at 100 m AGL. In large areas, wind speeds are lower by around 0.1 m/s. Therefore, no marked changes of wind speed are apparent. The significance of wind speed changes over the decades is quantified using statistical analysis as follows,

$$t = \frac{\bar{x}_1 + \bar{x}_2}{s\sqrt{\frac{1}{n_1} + \frac{1}{n_2}}} \quad (5)$$

where \bar{x}_1 is surface wind speed during 1961-1970. \bar{x}_2 is surface wind speed during 1991-2000. n_1 is number of data for group \bar{x}_1 and n_2 is number of data for group \bar{x}_2 . Calculation results by equation (5) shows that calculated value is 0.564739 and table value is 2.10; $(-2.10 < 0.564739 < 2.10)$, meaning that the differences of surface wind speed between 1961-1970 and 1991-2000 are not significant.

Table 2 shows annual wind field properties: average, standard deviation, minimum, and maximum values of the annual average wind speed from 1961 to 2000 at 30 m AGL at five observation points and ERA40 at 850 hPa. The highest of annual average surface wind speed during 1961-2000 is found in Aoyama of 6.31 m/s and the lowest is observed in Nagoya of 3.36 m/s. The standard deviation of annual wind speed is less than 10%, indicating that annual average wind speed has not fluctuated so much during the last three decades.

In summer, the highest surface wind speed is 6.00 m/s in Aoyama and the lowest is observed in Nagoya at 3.25 m/s

(see Table 3). In winter, the highest wind speed is found in Irago at 6.88 m/s and lowest is observed in Nagoya at 3.52 m/s (see Table 4). The surface wind speed in winter is more prominent than in summer since the Siberian high pressure system extends over the Japan isles during the winter season. The standard deviation of annual average surface wind speed is less than 0.10 m/s.

Table 2. Annual wind field properties during 1961–2000.

| Location | Average (m/s) | Standard Deviation (m/s) | Maximum (m/s) | Minimum (m/s) |
|----------|---------------|--------------------------|---------------|---------------|
| 850hPa | 7.87 | 0.14 | 8.87 | 7.14 |
| Aoyama | 6.31 | 0.02 | 6.76 | 6.11 |
| Irigo | 6.02 | 0.04 | 6.52 | 5.68 |
| Nagoya | 3.36 | 0.00 | 3.51 | 3.30 |
| Tsu | 4.40 | 0.01 | 4.72 | 4.26 |
| Tsuruga | 4.75 | 0.02 | 5.09 | 4.49 |

Table 3. Wind field properties in summer (April–September), 1961–2000.

| Location | Average (m/s) | Standard Deviation (m/s) | Maximum (m/s) | Minimum (m/s) |
|----------|---------------|--------------------------|---------------|---------------|
| 850hPa | 6.86 | 0.23 | 7.81 | 5.81 |
| Aoyama | 6.00 | 0.03 | 6.50 | 5.56 |
| Irigo | 5.41 | 0.06 | 6.06 | 4.86 |
| Nagoya | 3.25 | 0.00 | 3.42 | 3.11 |
| Tsu | 4.22 | 0.01 | 4.56 | 3.92 |
| Tsuruga | 4.41 | 0.03 | 4.81 | 4.12 |

Table 4. Wind field properties in winter (October–March), 1961–2000.

| Location | Average (m/s) | Standard Deviation (m/s) | Maximum (m/s) | Minimum (m/s) |
|----------|---------------|--------------------------|---------------|---------------|
| 850hPa | 9.28 | 0.24 | 10.74 | 8.08 |
| Aoyama | 6.74 | 0.04 | 7.11 | 6.30 |
| Irigo | 6.88 | 0.09 | 7.48 | 6.14 |
| Nagoya | 3.52 | 0.00 | 3.64 | 3.36 |
| Tsu | 4.67 | 0.02 | 4.94 | 4.38 |
| Tsuruga | 5.22 | 0.04 | 5.65 | 4.75 |

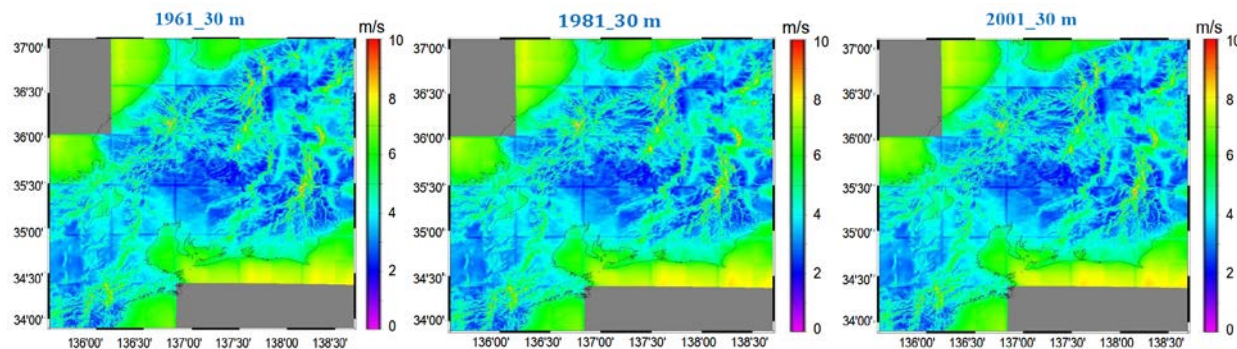


Figure 6. Spatial distributions of annual average wind speed at 30 m AGL in 1961, 1981, and 2001.

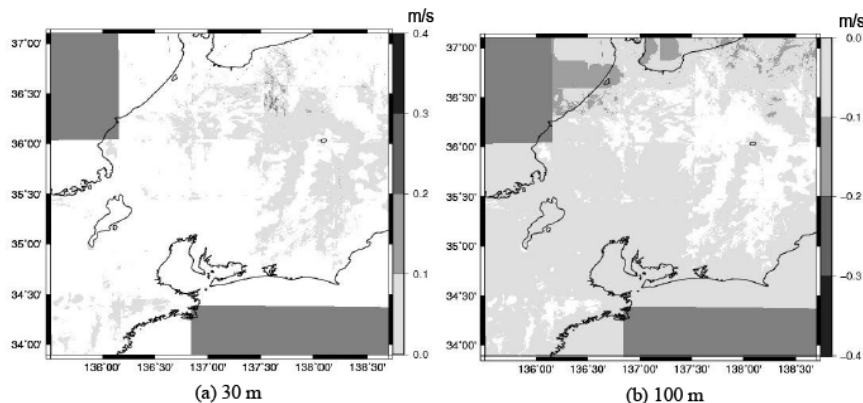


Figure 7. Spatial differences of average wind speed between 1961-1970 and 1991-2000 at 30 m and 100 m AGL.

To ascertain the effects of global warming on surface wind speed changes, we introduce the ratio $R_{\bar{V}}$ of average wind speed change as follows,

$$R_{\bar{V}} = \frac{\bar{V}_{1991-2000}}{\bar{V}_{1961-1970}} \quad (6)$$

where $\bar{V}_{1991-2000}$ and $\bar{V}_{1961-1970}$ are the surface wind speeds averaged during 1991-2000 (present climate) and 1961-1970 (past climate), respectively. If the ratio $R_{\bar{V}}$ based on the calculation of equation (6) is equal to 1.0, it follows that the changes of surface wind speed during 1961-2000 are not apparent in the Chubu area (Central Japan) and there is no significant effect of global warming on surface wind speed during the late 20th century. Figure 8 shows the frequency distribution of the ratio of wind speed change $R_{\bar{V}}$. The increase of annual wind speed is not apparent because the average value of $R_{\bar{V}}$ is just 1.0.

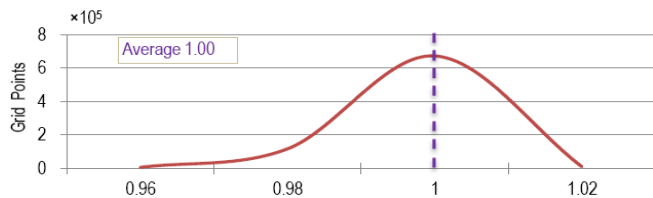


Figure 8. Ratio of average surface wind speed between 1961-1970 and 1991-2000.

Figure 9 shows the time series of the annual wind speed at the 850-hPa level projected by CMIP3 during 2001-2099. Annual wind speeds remain stable from 2001 to 2020 with the value at around 8 m/s. The surface wind speed slightly fluctuates by 1 m/s during 2021-2045, with the highest wind speed of about 8.5 m/s and the lowest of about 7.7 m/s. During 2046-2099, surface wind speed fluctuations occur within the limits of 8.0 m/s to 9.0 m/s. The annual average wind speed shows a gradual increase in linear trend with fluctuating by about 0.2 m/s year by year. The average wind speed is around 8 m/s during 2001-2046, although it is greater than 8 m/s during

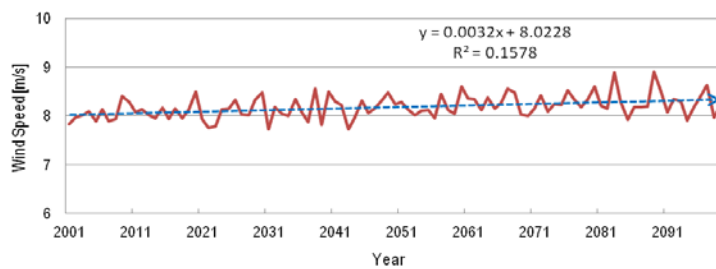


Figure 9. Time series of annual wind speed at the height of 850 hPa in point 35.0°N, 137.5°E.

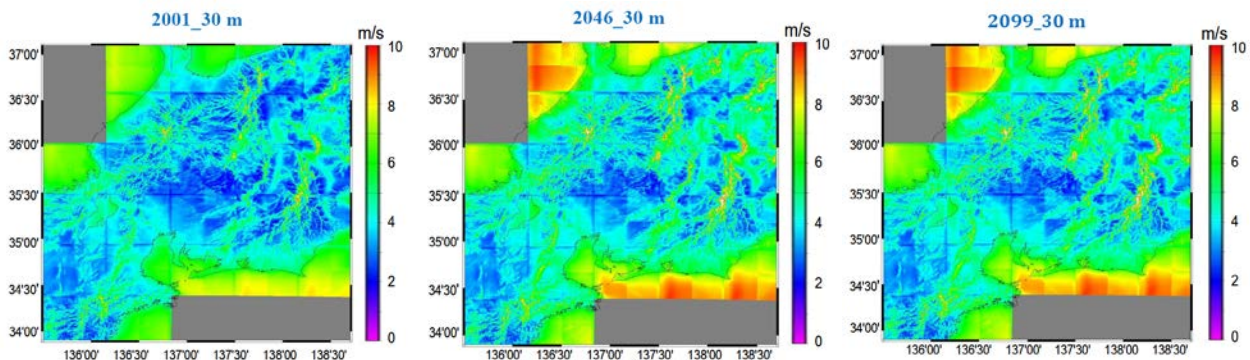


Figure 10. Spatial distributions of annual average wind speed at 30 m AGL in 2001, 2046, and 2099.

2046-2099. For 2081-2091, the highest wind speed is almost as high as 9 m/s. The wind speed trend increases continuously after 2000, meaning that future global warming can influence annual wind speed at the 850-hPa level over a long period of years.

Table 5. Domain-averaged wind speed differences at 30 m AGL.

| Year | 2046 | 2064 | 2099 |
|----------------------------------|----------|----------|----------|
| Increase of wind speed from 2001 | 0.57 m/s | 0.50 m/s | 0.48 m/s |

Figure 10 portrays the spatial distributions of the annual average wind speed at 30 m AGL in 2001, 2046, and 2099, estimated by GWA333, ERA40 and CMIP3. In these figures, blue colors denote lower wind speed. Generally, the highest annual wind speed field is found in coastal and mountain areas with the value of about 8 m/s in 2001 and 10 m/s in 2099, indicating that the future climate change might strongly affect the surface wind field especially in coastal and mountainous regions. Comparison reveals that annual wind speeds in 2046 and 2099 are greater than those in 2001, as confirmed by widespread yellow and red coloration of the images. The difference of annual wind speed between 2046 and 2099 is smaller than that between 2001 and 2046. This indicates that the increase of surface wind is almost completed by the middle of the 21st century, as a result of the global warming caused by the accumulated burning of fossil fuels in the early 21st century.

Table 5 shows the differences of the domain-averaged wind speed at 30 m AGL. If the annual average wind speed in 2001 is used as a basis of comparison, then upcoming global warming completes the modification of the surface wind field in nearly all areas in Central Japan by the middle of the 21st century. The greatest increase in wind speed occurs during 2001-2046, and the difference of wind speed after 2046 is not so significant. Under the SRES A1B scenario, change of surface wind attributable to future global warming becomes maximum during 2001-2046. Table 6 presents the numbers of grid points of the annual wind speeds that exceed 5 m/s, 8 m/s, and 10 m/s at 30 m and 100 m AGL. It indicates that areas with wind speed of 5 m/s, 8 m/s and 10 m/s increase in 2046 and 2099 compared with 2001 at both 30 m and 100 m AGL, and the highest increase is likely to occur by 2046. Increase of wind speed is greater at 100 m AGL than that at 30 m AGL.

Table 6. The numbers of grid points of the annual wind speeds that exceed 5 m/s, 8 m/s, and 10 m/s at 30 m and 100 m AGL.

| Year | 30 m AGL | | | 100 m AGL | | |
|------|---------------------|-------------------|------------------|---------------------|---------------------|-------------------|
| | >5 m/s | >8 m/s | >10 m/s | >5 m/s | >8 m/s | >10 m/s |
| 2001 | 243,518 (30.06%) | 7,801 (0.96%) | 379 (0.05%) | 482,856 (59.61%) | 54,211 (6.69%) | 1,698 (0.21%) |
| 2046 | 332,530 (41.05%) | 67,098 (8.28%) | 1,754 (0.22%) | 595,501 (73.52%) | 130,291 (16.09%) | 13,632 (1.68%) |
| 2099 | 318,185 (39.28%) | 60,422 (7.46%) | 1,638 (0.20%) | 573,283 (70.78%) | 114,655 (14.15%) | 6,738 (0.83%) |

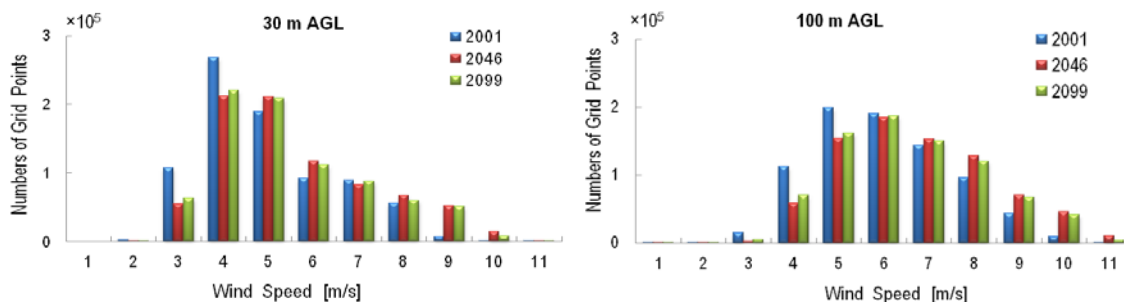
**Figure 11.** Frequency distributions of annual average wind speeds at 30 m and 100 m AGL.

Figure 11 shows frequency distributions of annual average wind speeds at 30 m and 100 m AGL in 2001, 2046, and 2099. At 100 m AGL, the areas with a wind speed of 6 m/s or lower are wider in 2001 than in 2046 and 2099, but areas with a wind speed of over 6 m/s are more predominant in 2046 and 2099 than in 2001. The frequency distribution shows the maximum at around 5 m/s in 2001, but around 6 m/s in 2046 and 2099. The same tendency can be seen at 30 m AGL. The frequency distribution exhibits the maximum at 4 m/s in 2001, but around 4-5 m/s in 2046 and 2099. Although the peak of the frequency distribution in 2001 is almost same as that in 2046 and 2099, the areas wind speed more than 9 m/s are enlarged significantly after the middle of the 21st century.

Wind speed is higher in winter compared with in summer during 1961-2000 (Table 3 and 4). Wind speed differs in each location depending on the land surface types and topographical conditions; coastal areas and mountainous regions may have larger impact on surface wind speeds (Figures 4, 6, and 10). Changes of surface wind speed in Central Japan have yet to appear during 1961-2000 and the global warming has little effect on the surface wind speed as of the late 20th century (Figures 5-8). The surface wind speed might increase continuously after 2000 until the early 21st century (Figures 9 and 10). Wind speed in 2046 and 2099 exceeds the wind speed in 2001. Over the coastal and mountainous regions, the wind speed at 30 m AGL increases from 8 m/s in 2001 to 10 m/s in 2099 (Figure 10), and the differences of wind speed distributions between 2046 and 2099 are not so significant (Table 5). The areas with a wind speed of over 7 m/s are larger in 2046 and 2099 than those in 2001 at both 30 m and 100 m AGL (Table 6 and Figure 11). In general, wind power generation is mainly influenced by the surface wind speed, so that the future climate change could be expected to enhance the potential of wind energy in Central Japan.

4. Conclusion

Wind speed differs in each area depending on the land surface and topographical conditions, the highest annual wind speed is found in mountain and coastal areas. Increases and decreases of surface wind speeds in Central Japan are not found during 1961-2000, but the wind speeds are predicted to increase during 2001-2099. Changes of surface winds because of global warming will be at its greatest during 2001-2046.

The differences of wind speed distribution between

those in 2046 and 2099 are small, and wind speeds in 2046 and 2099 are expected to exceed the wind speed in 2001. Over the coastal and mountainous regions, the wind speed at 30 m AGL increases from 8 m/s in 2001 to 10 m/s in 2099. The areas with a wind speed of over 7 m/s are larger in 2046 and 2099 than those in 2001 at both 30 m and 100 m AGL. Therefore, if global warming advances following the IPCC A1B scenario, then the wind speed in Central Japan is expected to increase.

References

- [1] International Energy Agency, *World energy outlook 2004* (2004) OECD/IEA, Paris, France, <http://www.worldenergyoutlook.org/media/weowebiste/2008-1994/WEO2004.pdf>.
- [2] Mondal, AHMd, Denich M, Assessment of renewable energy resources potential for electricity generation in Bangladesh, *Renewable and Sustainable Energy Reviews* 14 (2010) 2401-2413.
- [3] International Energy Agency, *World energy outlook 2007* (2007) OECD/IEA, Paris, France, <http://www.iea.org/textbase/npsum/weo2007sum.pdf>.
- [4] United Nations, *Kyoto protocol to the United Nations framework convention on climate change* (1998) <http://unfccc.int/resource/docs/convkp/kpeng.pdf>.
- [5] Delucchi MA, Jacobson MZ, Providing all global energy with wind, water, and solar power, Part II: Reliability, system and transmission costs, and policies, *Journal of Energy Policy* 39 (2011) 1170-1190.
- [6] Tan SBK, Shuy EB, Chua LHC, Modeling hourly and daily open-water evaporation rates in areas with an equatorial climate, *Hydrological Processes* 21 (2007) 486-499.
- [7] Sesto E, Ancona DF, Present and prospective role of wind energy in electricity supply, *Proc. of New Electricity 21: Designing a Sustainable Electric System for the Twenty-First Century* (1995) OECD Publications, Paris, France.
- [8] Keyhani A, Varnamkhasti AG, Khanali M, Abbaszadeh R, An assessment of wind energy potential as a power generation source in the capital of Iran, Tehran, *Journal of Energy* 35 (2010) 188-201.
- [9] Sesto E, Casale C, Exploitation of wind as an energy source to meet the world's electricity demand, *Journal of Wind Engineering and Industrial Aerodynamics* 74-76 (1998) 375-387.
- [10] Pryor SC, Barthelmie RJ, Climate change impacts on wind

- energy: A review, *Renewable and Sustainable Energy Reviews* 14 (2010) 430-437.
- [11] Ren D, Effects of global warming on wind energy availability, *Journal of Renewable and Sustainable Energy* 2-052301 (2010) 1-5.
- [12] Diamond KE, Global Warming's Impact on Wind Speeds: Long-Term Risks for Wind Farms May Impact Guarantees and Wind Derivatives Tied to Wind Energy Production, 40th Annual Conference on Environmental Law 2011 Salt Lake City, UT.
<http://www.lowenstein.com/publications/articles/List.aspx?view=rest>.
- [13] Sailor DJ, Smith M, Hart M, Climate change implications for wind power resources in the Northwest United States, *Renewable Energy* 33 (2008) 2393-2406.
- [14] Yoshino J, Takeuchi H, Shimada S, Yasuda T, Development and verification of the wide-area long-term high-resolution wind simulation system, *Wind Energy* 31/4 (2007) 115-122.
- [15] Uppala SM, et al., The ERA-40 re-analysis, *Quarterly Journal of the Royal Meteorological Society* 131 (2005) 2961-3012.
- [16] Meehl GA, Covey C, Delworth T, Latif M, McAvaney B, Mitchell JFB, Stouffer RJ, Taylor KE, The WCRP CMIP3 multi-model dataset: A new era in climate change research, *Bulletin of the American Meteorological Society* 88 (2007) 1383-1394.
- [17] Taylor, Karl, Program for Climate Model Diagnosis and Intercomparison, World Climate Research Program's (WCRP's) Coupled Model Intercomparison Project phase 3 (CMIP3) multi-model dataset,
http://badc.nerc.ac.uk/view/badc.nerc.ac.uk__ATOM__DE_23d41a54-d790-11df-a23a-00e081470265.
- [18] Dudhia J, A nonhydrostatic version of the Penn State/NCAR mesoscale model: validation tests and simulation of an Atlantic cyclone and cold front, *Monthly Weather Review* 121 (1993) 1493-1513.